Accepted Manuscript

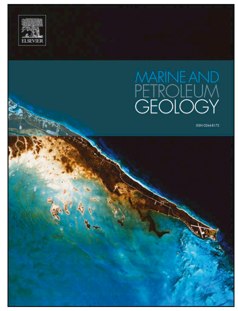

Quantifying tabularity of turbidite beds and its relationship to the inferred degree of basin confinement

Lilla Tőkés, Marco Patacci

PII: S0264-8172(18)30255-1

DOI: 10.1016/j.marpetgeo.2018.06.012

Reference: JMPG 3381

To appear in: *Marine and Petroleum Geology*

Received Date: 6 February 2018

Revised Date: 8 June 2018

Accepted Date: 11 June 2018

Please cite this article as: Tőkés, L., Patacci, M., Quantifying tabularity of turbidite beds and its relationship to the inferred degree of basin confinement, *Marine and Petroleum Geology* (2018), doi: 10.1016/j.marpetgeo.2018.06.012.

Quantifying tabularity of turbidite beds and its relationship to the inferred degree of basin confinement

Lilla Tokes[a] (Lilla Tőkés), Marco Patacci[b]

[a] Department of Physical and Applied Geology, Eötvös Loránd University, Pázmány Péter sétány 1/c, Budapest 1117, Hungary

[b] School of Earth and Environment, University of Leeds, Leeds LS2 9JT, UK

corresponding author: Lilla Tokes, lillatks@caesar.elte.hu

Abstract

Tabular beds and sheet-like deposits in deep-water systems have been the subject of much research attention; they can form high quality hydrocarbon reservoirs, owing to their excellent lateral continuity and predictable geometry. Additionally, deposit tabularity is a piece of evidence used to infer flow confinement in ancient systems and thus to evaluate the suitability of outcrop datasets as reservoir analogues. However, the quantification of tabularity is rarely attempted and a consistent definition on how to describe it quantitatively is lacking. For this study, published data from eighteen well-constrained ancient turbidite systems in outcrop were analysed. A simple and novel methodology for the quantitative calculation of tabularity along a transect from log panels and photo panels was devised, based on: a) subdividing beds into two groups based on their thickness, b) calculating the percentage of beds continuous across a fixed window (500m) and c) calculating the rate of thinning for the continuous beds within the same window. Calculations obtained from multiple locations within individual systems enable the investigation of proximal to distal, and axial to lateral changes in tabularity to be captured, and therefore permits the evaluation of tabularity in three-dimensions. A comparison between tabularity of the considered systems and their inferred degree of basin confinement shows that in the confined systems >90% of beds are continuous over 500m compared to <40% for the two

unconfined systems studied. In addition, different bed types were compared: hybrid event bed thinning rates are shown to be up to three times those of classical turbidites. This methodology provides a new tool to compare tabularity within and between systems quantitatively. It is hoped that the quantitative determination of tabularity will become a common workflow when describing ancient turbidite systems. It is suggested that this approach will enhance the value of outcrop data to inform models capturing the architecture of systems analogous to subsurface hydrocarbon reservoirs.

Keywords: sheet sands, bed continuity, bed thinning, confined turbidites, ponding, reservoir architecture

1. Introduction

Deep-water sediment gravity flow deposits can be described by their facies associations and by their internal architecture. At the simplest hierarchical level, depositional architecture is defined as the geometry of the individual beds or bedsets (Campbell, 1967): from very lenticular to tabular. Tabular beds typically form sheet-like deposits, which are recognised 'if individual beds in the deep-water succession can be traced for many tens of kilometres with no perceptible change in average bed thickness' (Pickering and Hiscott, 2015).

'Tabular' or 'sheet-like' can be used as a geometrical description of beds or bedsets, or as an architectural term (e.g. 'sheet sands'; Weimer and Slatt, 2006), referring only to bedsets or to entire hydrocarbon reservoirs. The internal architecture of the sheet is implied by describing them as amalgamated or layered sheets, defined on the preservation of mudstone layers between the individual sandstone beds (Chapin et al., 1994; Prather et al., 1998; Booth et al., 2000; Carr and Gardner, 2000; Johnson et al., 2001; Weimer and Slatt, 2006; Lomas et al., 2007; Etienne et al., 2013). Most studies describe the tabularity of bedsets (Slatt et al., 2000; Johnson et al., 2001; Weimer and Slatt, 2006), while individual bed tabularity is usually considered in high resolution studies dealing with beds that are continuous for several kilometres. The farthest correlations (100s km) are known from modern systems (Hieke and Werner, 2000; Nelson et al., 2000; Stevenson et al., 2013; Patton et al., 2015), while outcrop studies describe bed tabularity in relatively smaller ancient systems: e.g. Cerro Torro, Chile (Campion et al., 2011; Liu et al., 2018), Laingsburg Karoo, South Africa (Brunt et al., 2013), Tanqua Karoo, South Africa (Spychala et al., 2015), Peri-Adriatic basin, Italy (Di Celma et al., 2013), Gottero, Italy (Fonnesu et al., 2018), San Clemente, California (Li et al., 2016), which are the focus of this paper.

Tabular and lobate depositional forms are either used as contrasting geometries or as synonyms and their definition can be based on cross section or plan form geometries, or both. In cross section, a deposit with planar lower and upper surfaces is considered tabular, while a deposit with planar lower and mounded upper surfaces is often described as lobate (e.g. Johnson et al., 2001). In plan view, lobes are recognised on sea-floor images and high-frequency seismic based on their lobate, distributary or dendritic forms (Weimer and Slatt, 2006). Lobes are described from unconfined (Hodgson et al., 2006; Terlaky et al., 2016) and confined settings (Fig. 1A,B; e.g. Etienne et al., 2012; Marini et al., 2015). In some cases, the observed architecture of bedsets is described as sheet-form, which is, in turn, interpreted as the component of a lobe, several lobes or a fan (Carr and Gardner, 2000; Johnson et al., 2001; Hodgson et al., 2006). In a similar manner, sheet-like architectural elements, e.g. splays, can also make up lobes (Saller et al., 2008). The geometry of individual beds influences the stacking pattern of the bedset as well: tabular beds create aggradational stacking, lobate beds are more prone to stack compensationally (Liu et al., 2018).

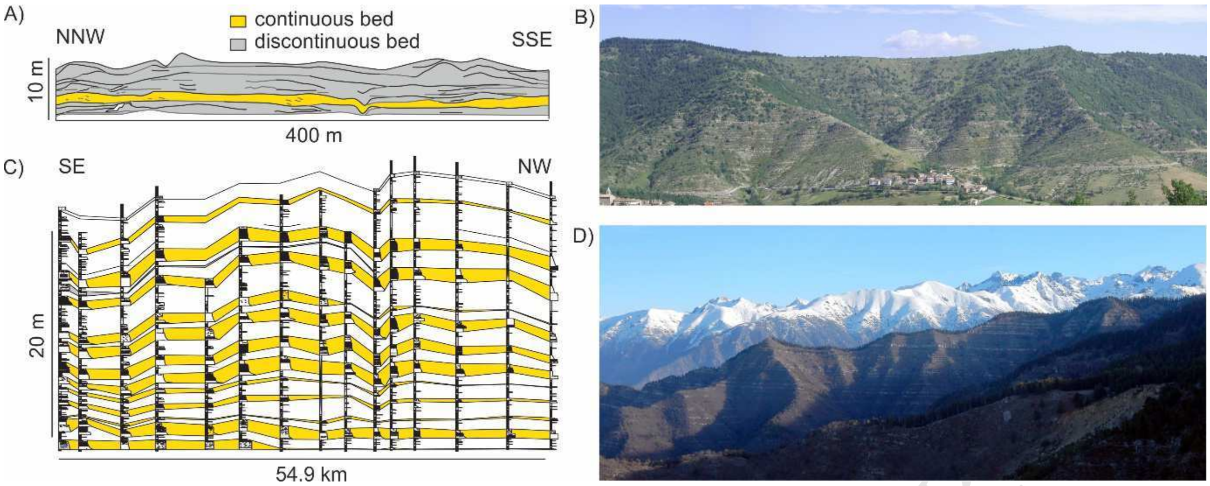

Figure 1 Outcrop examples of highly continuous beds with little change in thickness, i.e. tabular beds. A) Lobe-scale correlation panel of 'homogenous tabular and very extensive' sheet-sands from the Lauzanier sub-basin of the Annot System, France. Low bed continuity is attributed to the highly amalgamated and erosive nature of the deposit. Figure modified after Etienne et al., (2012); authors' interpretation shown as black lines, additional inferred amalgamation surfaces shown as grey lines. B) Lobes of Monte Bilanciere (looking towards NNW, view is around 1.2 km wide and 300 m high), comprising high continuity beds (many continuous for >10 km) from the Laga Basin, central Italy (see Marini et al., 2011; 2015). C) Bed-by-bed correlation panel 54.9 km long; transect parallel to palaeoflow (Marnoso-arenacea formation, Italy; modified after Amy and Talling, 2006). D) Confined high net-to-gross sheet sandstones (ridge in middle ground; looking towards NNW, view is around 2 km wide); Peïra Cava, Annot System, France (see Amy et al., 2007).

Basin-wide turbidite beds with parallel bounding surfaces at outcrop have been principally interpreted as basin-plain or as confined basin-plain settings (Mutti, 1977; Ricci Lucchi and Valmori, 1980; Pickering and Hiscott, 1985; Remacha and Fernández, 2003; Fonnesu et al., 2016). Unit 3 of the Marnoso-arenacea Formation of central Italy records the farthest individually correlated beds at outcrop, continuous for 120 km (Fig. 1C; Ricci Lucchi and Valmori, 1980; Amy and Talling, 2006; Muzzi Magalhaes and Tinterri, 2010). Sheet-like bed geometry and bed correlations in the range of tens of km are also characteristic of the Cloridorme Formation, Canada (Pickering and Hiscott, 1985; Awadallah and Hiscott, 2004) and of the Hecho Group of the Southern Pyrenees (Remacha and Fernández, 2003). While only few outcrop examples allow for correlations over 10s of km scale, systems where beds are continuous for a few kilometres are common (Fig. 1B,D; e.g. Kneller and McCaffrey, 1999; Amy et al., 2007; Haughton, 2001; Fonnesu et al., 2015; 2018; Marini et al., 2011, 2015, 2016a). It should be noted that tabular bed geometries are also described on the basis of outcrops and correlations from a few 10s to 100s of metres long (Elliott, 2000; Slatt et al., 2000; Mueller et al., 2017).

Tabular sheet sands have been the subject of much research attention as they are regarded as a primary component of high quality hydrocarbon reservoirs, owing to their excellent lateral continuity, predictable geometry and general well sorting (Weimer and Slatt, 2006). Examples of hydrocarbon reservoirs characterised by sheet sands can be found in the intraslope minibasins of the Gulf of Mexico (Prather et al., 1998; Booth et al., 2003) or in the Campos Basin, offshore Brazil (Bruhn and Walker, 1995; Albertão et al., 2011).

However, despite its academic and applied significance, quantitative characterisation of bed geometries and of their degree tabularity is only rarely attempted (e.g. Pickering and Hilton, 1998; Amy et al., 2000; Liu et al., 2018). This study proposes a methodology for the quantitative characterisation of bed tabularity and illustrates some of its applications by contrasting systems with different interpreted degree of basin confinement and by looking at different types of gravity flow deposits.

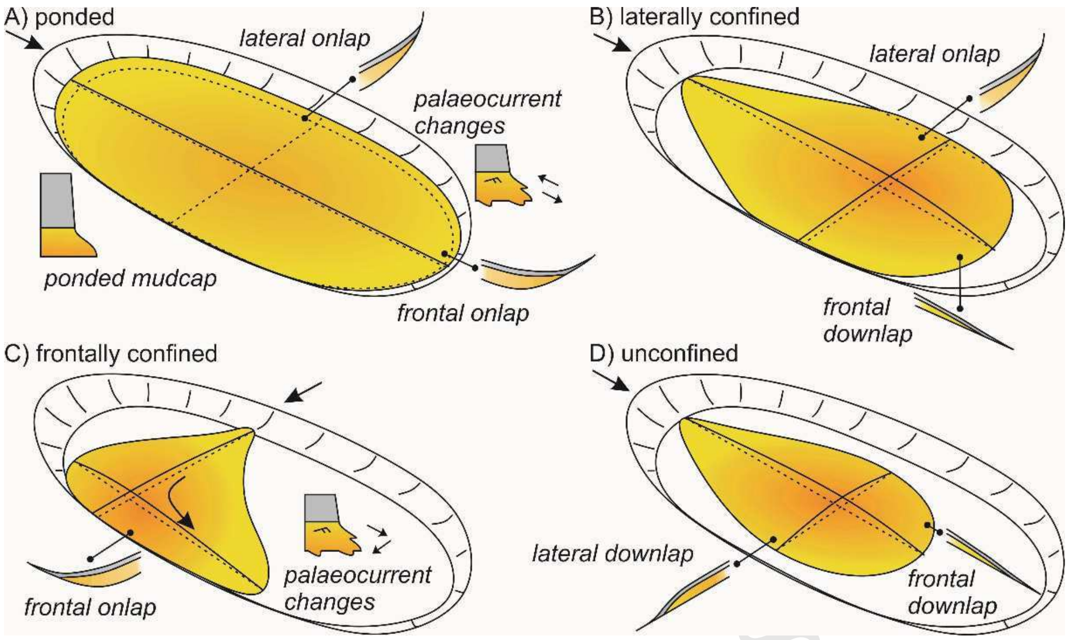

Figure 2 Different types of confinement: A) ponded, B) laterally, C) frontally confined, and D) unconfined flow deposits. The ratio between lobe size and basin size, the aspect ratio of the basin, and the sediment entry point are the major controls on the type and degree of confinement. Evidence for confinement comes from a range of observations in the rock record (in italics), including facies trends and bed geometries (not shown).

1.1. Deposit tabularity and flow confinement

Deposit tabularity is one of the pieces of evidence used to infer flow confinement (Ricci Lucchi and Valmori, 1980; Drinkwater and Pickering, 2001; Sinclair and Tomasso, 2002; Cornamusini, 2004; Lomas et al., 2007; Spychala et al., 2015). In this paper, the term 'confinement' is restricted to externally driven bathymetric confinement, hence lateral confinement in channel or canyon environments (e.g. degree of confinement of Brunt et al., 2013 and Labourdette and Bez, 2010) is not included. In its simplest formulation, the degree of confinement (cf. 'effective confinement' of Brunt et al., 2004) can be expressed as the relationship between the size of a lobe and the size of the basin. If the lobe size exceeds the basin area, the system is ponded (Fig. 2A), if the lobe is smaller than the basin, the system is unconfined (Fig. 2D). However, geometrical relations, i.e. the aspect ratio of the basin and its relation to the sediment entry point can add additional complexity resulting in a system that is frontally or laterally confined, but not ponded (Fig. 2B,C). Additionally, the term confinement can be used in reference to a variety of scales; from grain size classes within a single flow event (e.g. confinement of the lower, more sand-prone, coarser grained component of a stratified flow), to the entire flow event, or the entire depositional system and therefore additional complexity could be added to Figure 2. Finally, the considerable variability in the 3D geometry of basins (e.g. confining slopes height and shape) and in the expected shape of unconfined deposits from different flow types and volumes ensures that there is no agreed simple definition of the types (or degrees) of confinement.

At outcrop, determining the degree of confinement of ancient systems relies on a number of pieces of evidence in addition to deposit tabularity, such as mudcap thickness, onlapping relationships, palaeocurrent direction and distinctive facies changes (Fig. 2). Of these, onlapping relationships are the only objective feature that is common to all confined basins described in the literature (e.g. Prather et al, 1998; Smith and Joseph, 2004; Tinterri and Tagliaferri, 2015). Determining the degree of confinement in a more objective way could only work in modern settings, where basin area and sediment volume can be measured or estimated; something that cannot be fully ascertained in ancient settings, e.g. the basin size is usually a minimum estimate based on outcrop extent. In addition, the shape of confined basins is highly diverse and depending on their structural evolution, it might evolve through time, making their classification even more difficult. For example, the aspect ratio, tortuosity of the basin, dip of the basin floor and height of the confining slopes all control which part of the basin acts as a conduit for flows or as a depocentre.

The aims of this paper are to review the various definitions of tabularity, to propose a methodology to compare the degree of tabularity in different turbidite systems, to investigate the relationship between tabularity and inferred degree of confinement and to elucidate other controls on tabularity based on the analysis of data from a number of systems based upon the published literature.

2. Methods and data

Tabularity of deposits can refer to the external geometry of individual event beds or of bedsets (Fig. 3A), the latter being composed of several event beds. Bed tabularity commonly results in bedset tabularity, but a tabular bedset does not supply any information on its internal architecture, as individually discontinuous or strongly lenticular beds are possible components of a tabular bedset. Moreover, bedset tabularity can refer to a variable number of beds, usually defined on the basis of intervening mudstone intervals. Because of the way the term is loosely applied in literature, a common and objective definition based on hierarchical level, number of constituting beds or thickness of bedset cannot be easily established; for this reason, bedset tabularity is not considered in this study.

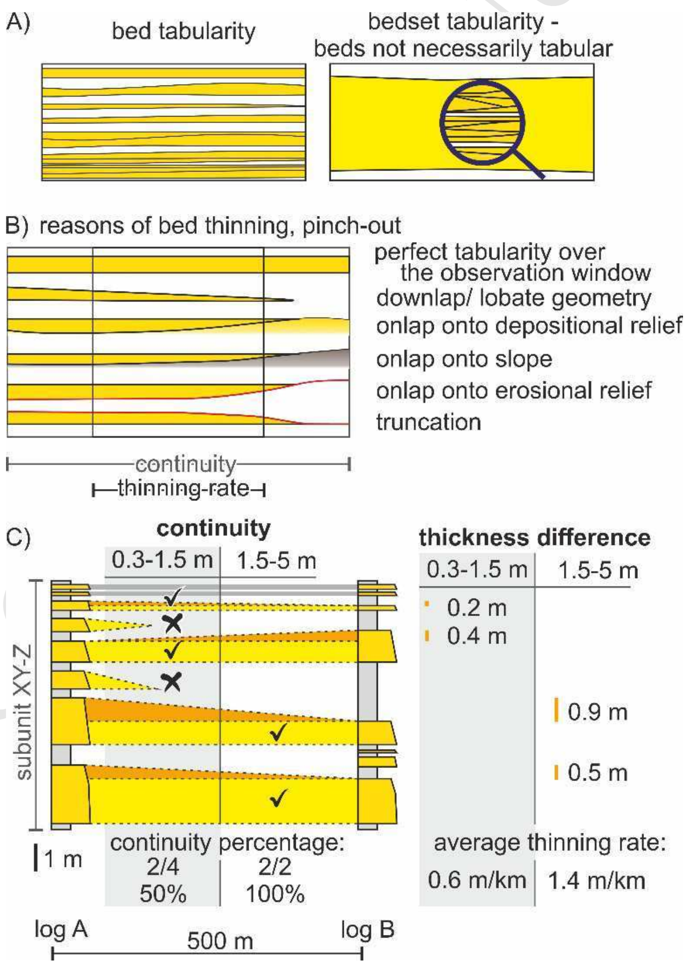

Figure 3 A) Types of tabularity. Along a transect, bed tabularity indicates the continuity of individual beds over a long distance with relatively little change in thickness. Amalgamated bed contacts are harder to

correlate than sand-mud bed contacts. Bedset tabularity generally refers to the correlatability and constant thickness of sandstone-rich units, which are made up of several event beds. They are described in the literature as tabular 'beds', units, packages, sheets or lobes. B) Reasons for bed thinning and pinching out. Positive depositional relief, lobate geometry results in downlap onto the substrate. Onlaps can be differentiated by the type of pre-depositional relief (e.g. an earlier depositional unit, a confining slope or an erosional surface). Erosional truncations also reduce bed tabularity. C) Methodology for tabularity quantification used in this study: sandstone beds in two logs, prefereably 500 m apart, were differentiated according to thickness ranges (e.g. 0.3-1.5 m and 1.5-5 m); for each range the percentage of continous beds over 500 m and the average thinning rate were calculated.

Bed continuity and thickness change can be related to a number of processes and geometrical constrains (Fig. 3B). The inherent finite lobate geometry of deposits of unconfined turbidity currents results in beds thinning and ultimately pinching out ('downlap'). Deposition from turbidity currents is usually thought to result in even thinning (Mutti, 1985; Sumner et al., 2012), however, abrupt thinning, especially of hybrid event beds or sandy debrites is also observed (Amy et al., 2005a; Amy et al., 2005b; Amy and Talling, 2006; Talling et al., 2012). The bathymetry of the basin floor can result in thinning and onlap of the beds; basin floor unevenness can be caused by previous depositional relief, by the presence of a basin margin, or by erosion caused by a previous event. Bed geometry can also be modified after deposition because of erosional truncation. Interplay of the above processes can occur, making it often difficult to differentiate the reasons for bed thinning and pinch-out.

2.1. Quantifying tabularity

Quantifying bed tabularity can be conducted in several ways, depending on the geometrical parameters used to define it and on the type of data available (e.g. 2D vs. 3D). The primary definition of tabularity is the highly continuous nature of the sandstone component of beds, hence quantifying sandstone bed continuity was taken as a first approach. Considering that most outcrop-based studies rely upon datasets that consist of 2D transects (e.g. log panels or photopanels), it was decided to devise a methodology based on this type of data. The most meaningful measure across a 2D transect would be the maximum extension of beds, where both terminations of a bed can be detected, however, this is rarely applicable in practice, bed dimensions commonly exceed the size of the available observation window. Bed continuity for a succession can also be expressed as the percentage of beds in a succession that are continuous over a certain distance. In a given succession, a steady increase in the size of the observation window results in no change in the proportion of beds that remain continuous, or a step-by-step decrease as the beds terminate laterally.

If beds are continuous within an observation window (500 m chosen for this study, see below), their degree of tabularity can be further defined by their change in thickness. The simplest quantification is comparing the thickness of the sandstone beds between two logs over the length of the window, thus neglecting internal, smaller scale thickness variations. The thickness change can be quantified either as absolute thinning, i.e. the absolute difference in bed thickness between the two logs, or relative thinning, i.e. the ratio between the difference of the two bed thicknesses and a measure of bed thickness (e.g. maximum or average). The absolute thinning rate can be also expressed as the 'angle of thinning', i.e. the angle formed with respect to the horizontal by the top of the bed, assuming a flat base, or vice versa. The absolute thinning rate can be normalised with respect to distance, enabling comparison when dealing with values calculated from logs separated by different distances. This is very useful, but by definition, thicker beds will inherently show higher absolute thinning rates than thinner beds having the same relative thinning rate. By considering beds of discrete thickness ranges separately, this limitation can be partly overcome. In contrast, relative thinning rate cannot be normalised for distance effectively, and the same bed with the same 'angle of thinning' will have different relative thinning rates at different locations.

In order to compare tabularity between different systems, a choice of standard parameters (e.g. the range of beds to include in the measurements and the size of the investigation window) was undertaken. All sandy bed types were included in the analysis (e.g. Bouma-type turbidites (Bouma, 1962), massive sandstone beds and hybrid event beds (Haughton et al., 2009)). Only the sandstone part of the beds was considered, therefore mudstone caps were not included in thickness measurements. This choice was dictated by the relative lack of published data on mudstone caps thickness and geometry in comparison to that of the sandstones. Although an evaluation of the tabularity of the mudstone caps and of combined sandstone-mudstone layers should prove very insightful, this would require a different approach to that proposed in this paper.

The beds were grouped into thickness ranges: distinct tabularity parameters were computed for medium-thickness beds (0.3-1.5 m) and thick beds (1.5-5 m). As measurements of tabularity always involve two logs, for classifying a bed into a thickness range, its greater thickness was used. Although the chosen thickness values are somehow arbitrary and alternative values (e.g. a lower boundary at 25 cm or the distinction between medium and thick beds at 1 m) could have been used instead, a number of considerations suggested this choice. First, thin beds (<0.3 m) could not be easily included as they are usually below the resolution of the correlations in many published log panels. Secondly it was necessary to divide the data into bed thickness classes as beds of different volumes might have been deposited by flows which had different interactions with the topography (confinement is a function of the ratio of flow volume to basin volume; see Fig. 2). The choice of creating two groups (rather than for example 3 or 4) was based on having as many bed measurements as possible in each group. By collecting more data, it might be possible to apply a similar methodology to that described in this paper with a larger number of bed thickness classes or to plot individual beds' tabularity against their thickness; however, this approach was beyond the scope of the present study. Finally, beds thicker than 5 m were excluded due to their very small number and exceptional flow volumes, resulting in a very small dataset from which summary statistics could not be reliably calculated.

The target distance between the two logs for continuity measurement was fixed at 500 m (Fig. 3C). This was chosen because it is a common correlation distance in published log panels and it represents a good compromise (between capturing the small scale variations and the large-scale ones) to cover the range of variations in tabularity in the depositional medial-to-distal domain of most ancient turbidite systems which represented the target dataset (proximal domains and submarine channel fills were not considered). The 500 m window is clearly an arbitrary width and transects in any direction in relation to palaeoflow were considered (see section 3.3 below for a discussion on transect orientation). As published logs display a wide range of distances, some flexibility on this criterion was necessary and logs separated by as little as 400 m or by as much as 600 m were included. In addition, logs further away than the fixed distance of 500 metres were used to provide minimum values of continuity (i.e. continuity for any smaller windows must always be equal or greater). The absolute thinning rate for each bed was calculated as the difference between the greater and smaller thickness of the correlated bed, divided by the distance between the two logs. The average for a dataset for each bed thickness group (0.3-1.5 m and 1.5-5 m) was calculated only if the sample size included at least 3 beds.

2.2. Limitations

As the measurement of tabularity is based on 2D transects, the calculated values can only give an indication on the three-dimensional tabularity of the beds. In addition, there are a number of 'technical' limitations of the method, attributable to the quality and resolution of the original data, of the interpretation and of the published figure. They can be grouped as being related to the vertical resolution, lateral resolution and bed correlation detail.

2.2.1. Vertical resolution

- Vertical resolution can be hindered by covered/vegetated intervals in outcrop; however, this is more typical of muddy or thin bedded intervals, therefore their impact on correlation and thickness trends of sandstone beds that are thicker than 30 cm is minor.
- Amalgamation can make distinguishing event beds from bedsets difficult and reduces the confidence of correlations.
- The accuracy of thickness measurements depends on the method applied. The error associated with outcrop sedimentary logging is often around or greater than 10% (e.g. see Patacci, 2016), so even a perfectly tabular bed might have some thickness variation due to measurement errors.
- Log panels are usually drawn at a lower resolution than the one they were measured at, and their resolution is sometimes further lowered when published.

2.2.2. Lateral resolution

Lateral resolution depends on the distance between logs, the number of available logs and the type of correlation.

- It is dependent on the maximum outcropping width of the system: most log panels do not show the entire system and only in some cases one side termination is exposed. The true length of beds thus cannot be ascertained.
- There is a tendency to publish correlation panels of outcrops with beds that correlate, rather than the opposite.
- Outcrop lateral continuity between logs can be an issue when estimating the percentage of beds that correlate; however, it is less so when calculating thinning rate, assuming that thinning rates (away from their pinchout) are relatively constant.

2.2.3. Bed correlation

Each bed correlation can be either observed, based on walking outor on a photopanel, where the location of pinch-outs is shown; or the correlation can be inferred, based only on bed thicknesses patterns and their sedimentological characters (e.g. hierarchical correlation of Remacha and Fernández, 2003 and Muzzi Magalhaes and Tinterri, 2010). The thinnest bed correlated will also affect the ability to compute accurate continuity statistics, and when only bedsets are correlated, instead of event beds, correlation of event beds is imprecise or not possible.

The requirement of a high vertical resolution and of the minimum distance between logs limit the type and number of suitable published log panels. There is a bias toward high continuity, ponded systems in tectonically active foreland basins. These are mainly medium- to coarse-grained sandy systems. Data from unconfined systems are only available from the relatively proximal part of some systems (Tanqua Karoo, Windermere). However, thick to very thick beds considered in this study are not expected in the more distal part of such systems and a direct comparison with modern unconfined and muddy systems is outside the scope of this study. Instead, the proximal versus distal and along-flow versus cross-flow transects in the same systems can be quantitatively compared (see section 3.3).

2.3. Inferred degree of confinement

To explore the relationship between the degree of tabularity and the degree of confinement, a review of the degree of confinement for each system (or unit) had to be carried out. First, the authors' original interpretation was recorded, together with the lines of evidence used to support it. As the terminology concerning the definition of the degree of confinement is not always consistent between different authors and can vary due to the purpose of the study or the type of dataset, a numeric "degree of confinement index" was also devised to make systems comparable. This index is based on the combination of the authors' interpretation and of the available evidence such as facies trends and palaeocurrents interpreted as indicative of confinement, onlap geometries and sandstone beds with thick mudstone caps.

Unconfined (C0): identified by all authors as "unconfined", there is no evidence for any kind of topographic confinement.

Confined (weak) (C1): defined "confined" by some or all authors, but only sandstone facies trends or palaeocurrent evidence.

Confined (C2): defined "confined" or "ponded" by all authors. Onlap geometries observed; evidence listed in (C1) might also be present; however, no characters specific to (C3) observed.

Ponded (C3): defined "confined" or "ponded" by all authors; sandstone beds with thick mudcaps; evidence listed in (C1) and (C2) might also be present. Thick mudstone deposits linked to the flow that deposited the sandstone beds are the result of flows that were trapped within the basin, the muddy suspension cloud filling the whole basin (Pickering & Hiscott, 1985; Haughton, 1994).

The confined (C2) code can also be assigned to a unit above or below a unit (C1) or (C3) when a trend of increasing/decreasing confinement is observed, even if onlap geometries are not recorded. Finally, it should be pointed out that beds or bedset tabularity, sandstone bed statistics (e.g. Felletti and Bersezio, 2010) or stacking patterns, which are linked with the common bed geometry, were not considered when assigning the degrees of confinement codes to avoid circular reasoning.

2.4. Datasets

Eighteen ancient turbidite systems were chosen for the study, based on availability of high-quality data (i.e. log correlation panels or interpreted photomontages) suitable for this type of analysis (Table 1). For each system, one or more units could be identified, based on those established by the authors. Average bed continuity and average bed thinning rates between two logs were calculated for intervals 40-80 m thick. The thickness of the intervals was chosen as the best compromise between accurate statistics (thick intervals = more beds = more accurate statistics) and capturing the system evolution (thin intervals = more intervals = better insight into vertical changes). In a few cases, when the available log panels were shorter than 40 m, intervals as short as 10 m where included. These intervals for each log pair are referred to as 'datasets' and are defined based on the stratigraphic position of the intervals and on the location of the log pairs used to calculate the metrics. Therefore, two datasets can represent different stratigraphic intervals at the same location or different locations (e.g. proximal and distal) of the same stratigraphic interval. Datasets can thus record the temporal evolution or spatial differences in the same unit. A total of 58 datasets including around 700 beds thicker than 30 cm (c. 500 beds 0.3-1.5 m; c. 200 beds 1.5-5 m) from 21 papers were considered.

Code	System	Unit	Basin type	Grain size	Data sources	Number of datasets (distance of logs in m)	Confinement: authors interpretation	Confinement: evidence (in addition to facies and bed geometry)	Confine-ment index	Sandstone architecture	Inferred basin area (km^2)
AL-C	Tabernas	Alfaro, Unit C	transtensional	medium	Baudouy, 2011	1 (455)	ponded	thick mudcaps, onlaps, palaeocurrents	3	laterally extensive sheets	30
BR	Annot, Annot sub-basin	Upper Braux	proforeland	coarse	Kneller and McCaffrey, 1999; Patacci et al., 2014	1 (800)	flows completely confined	onlaps, palaeocurrents	2	sheet architecture	160
CS-1	Castagnola	Unit 1	wedgetop	medium	Southern, 2015; Marini et al., 2016a	4 (2200)	ponded	thick mudcaps, onlaps, palaeocurrents	3	basin-wide tabular sand-mud couplets	24
CT-PC	Cerro Toro	Paine C, Phase 3	retroarc foreland	medium	Liu et al., 2018	1 (800)	confined slope; unconfined	onlap?	1	sandy lobe infill, not sheet-like beds	12
GC	Annot, Grand Coyer	S 1-3	proforeland	coarse	Clark et al., 2007	1 (500)	highly confined	-	1	amalgamated sheet sandstones	250
GT-3a	Gottero	Gottero 3a	trench-slope	medium	Fonnesu, 2016; Fonnesu et al., 2018	3 (660)	confined basin-plain	-	1	sheet-like, continuous beds	3500
GT-3b		Gottero 3b				4 (660)	transitional between confined and ponded	-	2		
GT-3c		Gottero 3c				2 (620)	ponded	thick mudcaps	3		
HC-B2	Hecho	Banastón-2	proforeland	fine	Remacha and Fernández, 2003	3 (8500, 9000, 9500)	ponded	thick mudcaps, palaeocurrents, onlaps	3	sheetlike lobe, basin-plain	4500
LN	Laingsburg Karoo	D/E, E1	intraslope	fine	Spychala et al., 2015	1 (500)	intraslope accommodation	palaeocurrents	1	tabular sand-prone units	1100
LG-1b	Laga	Crognaleto	proforeland	medium	Marini et al., 2015	8 (1650, 2500, 4750, 5500)	confined, but not ponded	onlaps, palaeocurrents	3	sheet-like lobes	1100
LG-2		Mt. Bilanciere				4 (2350, 2450)	semi-confined	onlaps	2	shingled-compensated lobes	1700
LL	Las Lajas	Stage III	palaeofjord	fine	Liu et al., 2018	1 (1000)	highly confined, ponded	onlaps, thick mudcaps	3	aggradational sheet sand system	5
LZ-L	Annot, Lauzanier	Lower Unit	proforeland	coarse	Etienne et al., 2012	2 (400, 500)	moderately confined, lobes	onlaps	1	sheet-sand	250
MA-IIIB	Marnoso-arenacea	Unit III-B	proforeland	fine	Amy and Talling, 2006; Tinterri and Tagliaferri, 2015	3 (2600, 5100, 5300)	lateral confinement; ponding	thick mudcaps, palaeocurrents	3	extensive bed continuity	4500
PC-1	Annot, Peïra Cava	Stage 1	proforeland	coarse	Amy, 2000	1 (2400)	ponded	thick mudcaps, onlaps	3	sheetform turbidites	250
PC-2		Stage 2				2 (500)	ponded	thick mudcaps, onlaps	3		
RS-M	Ross	Middle Ross	transtensional	very fine	Straub and Pyles, 2012	2 (430, 500)	structurally confined, 'ponded'	palaeocurrents	1	lobe elements	2700
SR-L	Sorbas	Lower Unit	transtensional	medium	Haughton, 1994, 2001	2 (675, 850)	ponded	thick mudcaps, palaeocurrents	3	sandstone sheets	100
SR-U		Upper Unit			Haughton, 2001	1 (950)	ponded	thick mudcaps, onlaps, palaeocurrents	3	ponded turbidite sheets	

TN-3	Tanqua Karoo	Fan 3	retroarc foreland	fine	Groenenberg et al., 2010	2 (500)	unconfined, lobe axis	-	0	sheet-like elements, lobes	5000
TS-2	Cerro Bola	TS2	retroarc foreland (disputed)	medium	Liu et al., 2018	2 (600, 620)	loosely confined	onlaps	2	lenticular beds with shifting depocentre	400
TS-4		TS4				2 (750, 1200)	moderately confined	onlaps, thick mudcaps	3	aggradational tabular beds	
WN-U	Windermere	Upper Kaza	passive margin	coarse	Terlaky et al., 2016; Terlaky and Arnott, 2014	5 (500, 600)	unconfined mid-fan, proximal basin floor	-	0	sheet-like basin floor elements	5000

Table 1 List of units considered in this paper. The confinement index aims to compare units based on evidence for basin confinement: 0: unconfined, 1: weakly confined; 2: confined; 3: ponded (see section 2.3 for definitions). Evidence for confinement does not include sedimentary facies and bed geometry. The codes are coloured as the respective datapoints on figures 4 and 5.

3. Results

Computed tabularity values for the analysed 58 datasets from 22 units are shown in Figure 4. Measurements for beds belonging to each of the two thickness ranges are plotted separately (0.3-1.5 m beds in Fig. 4A, B and 1.5-5 m beds in Fig. 4C, D). The four plots are arranged so that bed continuity (first order description of tabularity) is shown on the left (Fig. 4A, C), while the thinning rate is on the right side. Thinning rates are only shown for datasets where continuity is ≥90% and is used to capture variations in tabularity for highly-continuous datasets (Fig. 4B, D).

Both measurements of tabularity are plotted against net-to-gross (n:g), defined as the cumulative thickness of the sandstone intervals of any thickness divided by the total thickness. This was chosen because it is a quantitative descriptive parameter that combines information on the type of system (sandy vs muddy) and on the relative position within a system (proximal vs distal).

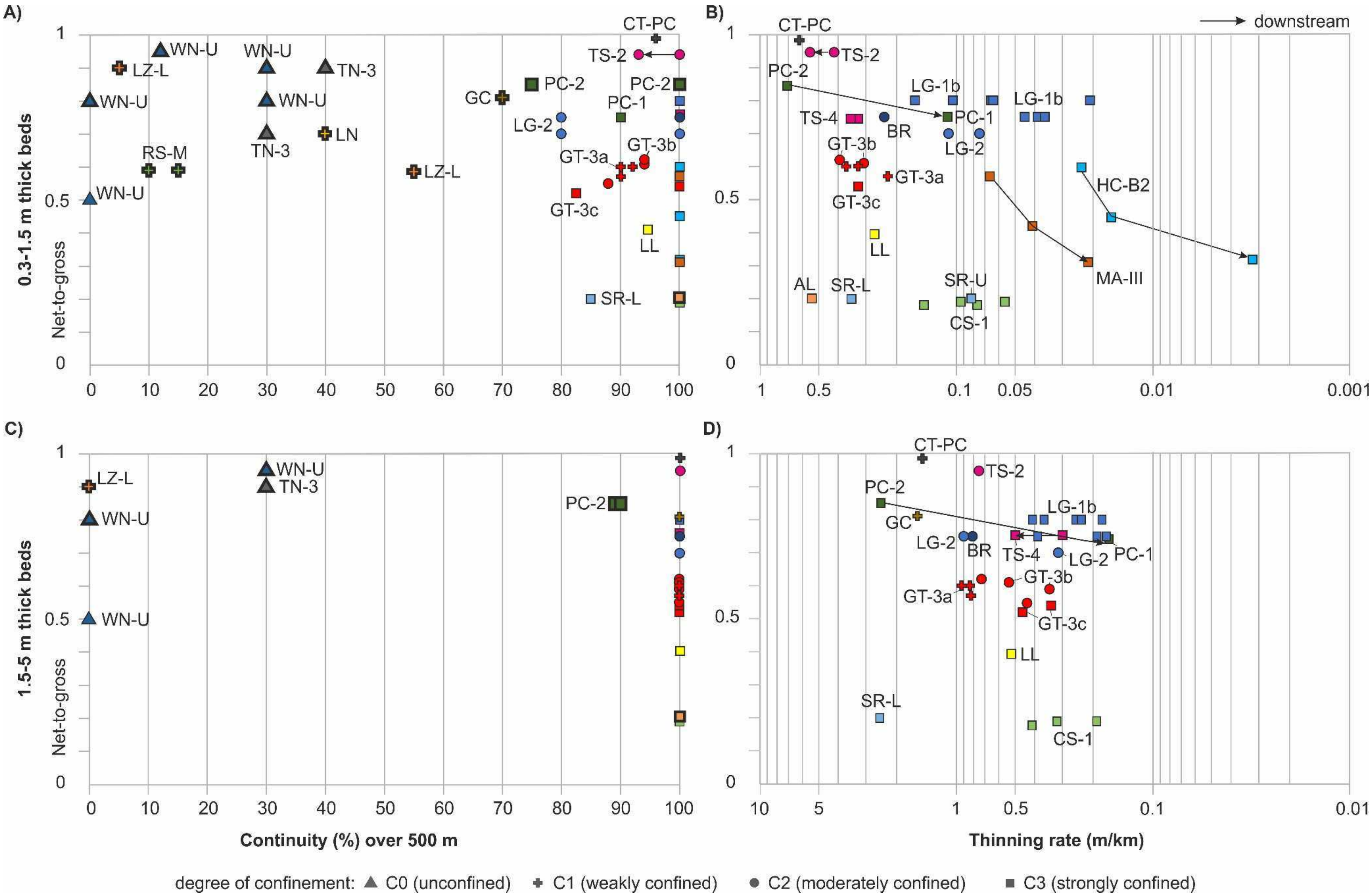
A)
B)
C)
D)
downstream
0.3-1.5 m thick beds
1.5-5 m thick beds
Net-to-gross
Continuity (%) over 500 m
Thinning rate (m/km)
CT-PC
TS-2
PC-2
PC-1
GC
LG-2
LG-1b
GT-3a
GT-3b
GT-3c
LL
SR-L
SR-U
WN-U
LZ-L
TN-3
LN
RS-M
TS-4
BR
HC-B2
MA-III
AL
CS-1
degree of confinement: C0 (unconfined) C1 (weakly confined) C2 (moderately confined) C3 (strongly confined)

1

Figure 4 (A,C) Percentage of continuous sandstone beds (continuity) and (B,D) their average thinning rates, calculated for each dataset. (A,B) Beds 0.3-1.5m thick and (C,D) beds 1.5-5m thick. Thinning rate is calculated for datasets where ≥90% beds are continuous. Continuity datapoints can represent exact values (bold edge) or minimum values (when calculated from correlation panels with distance > 500 m). Values are plotted against net-to-gross of the interval (sandstone thickness divided by total thickness). Symbols indicate the confinement index (see section 2.3 for definition). Each unit is illustrated by a different colour and identified by a code (see Table 1). Arrows show the relative position of individual datasets along dip.

3.1. Tabularity and inferred degree of confinement

Results suggest that in the considered examples continuity of 0.3-1.5 m beds over 500 m varies from 0 to 100% (Fig. 4A), while for 1.5-5 m beds two clusters can be observed (≤30% and ≥90%), with all but one of the confined cases (of any degree, 1-3) having a >90% continuity (Fig. 4C). The exception is the Lauzanier (LZ-L), interpreted as a confined system (confinement index, C1) and characterised by compensating proximal lobes (Etienne et al., 2012; Fig. 1A). Some units do not have beds 1.5-5 m thick (Ross RS-M, Laingsburg Karoo LN, Marnoso-arenacea MA-III, Hecho HC-B2), thus the relationship between thinner and thicker beds cannot be examined in their case.

Based on all 7 studied datasets, unconfined (confinement index, C0) systems have ≤40% continuity for beds of both thickness ranges (Fig. 4A,C). Weakly confined (C1) systems bear high variability in continuity, which can be related to the poor definition of 'weak confinement', or the variable position of where the data come from, e.g. the Ross (RS-M) and Laingsburg Karoo (LN) datasets are regarded as relatively proximal, while the Gottero 3a (GT-3a) as the distal part of the system. The Lauzanier is a good example of the variability in continuity within one unit, with a stratigraphically lower high net-to-gross dataset characterised by widespread bed amalgamation displaying only 5% continuity (Fig. 4A, section on Fig 1A), while a stratigraphically younger dataset dominated by heterolithic beds (0.6 n:g, Fig. 4A) having 55% continuity. Moderately (C2) and strongly (C3) confined systems show ≥80% continuity for 0.3-1.5 m and >85% for 1.5-5 m beds. In conclusion, the above observations suggest that in the chosen examples bed continuity over 500 m (1.5-5 m thick beds) is a good proxy for confinement. It should be noted that there is a bias towards confined, high continuity systems that are presented on at least 500 m long correlation panels in the literature.

A relationship between degree of confinement and thinning rate is more elusive. Figures 4B and 5A show thinning rates for beds 0.3-1.5 m thick with ≥90% and <90% continuity, respectively. The ranges of different degrees of confinement overlap; however, values of absolute thinning rate <0.07m/km are linked to strong (C3) confinement (Fig. 4B), while values >0.7m/km belong to low continuity weakly (C1) confined to unconfined (C0) settings (Fig. 5A). Weakly confined (C1) datasets show 0.2-0.7m/km thinning rates in high continuity cases, but thinning rate is as high as 3m/km in low continuity cases, such as the Lauzanier (LZ-L; Fig. 5A). Weakly (C2) confined 1.5-5 m beds thin between 0.8-1.6m/km, while 0.3-1m/km thinning rate characterises moderately, and 0.18-3m/km strongly (C3) confined settings. Laga moderately confined unit (C2: LG-2) has an average lower continuity in 0.3-1.5 m beds, and higher thinning rate for both bed thickness ranges than the Laga strongly confined (C3: LG-1b), but the two units overlap on all plots. Gottero weakly confined units (C1: GT-3a), dominated by lobe-like amalgamated sand-sheets (Fonnesu et al., 2018), plot close to each other, while moderately and strongly confined ones (C2, C3: GT-3b,c) display higher variability. Stratigraphic thinning rate trends of datasets are similar in the two thickness ranges. The four units described by Liu et al. (2018) show increasing tabularity and degrees of confinement according to their calculations in the following order: Cerro Toro Paine C member CT-PC (C2), Cerro Bola TS-2 (C2), Cerro Bola TS-4 (C3) and Las Lajas LL (C3). This is confirmed by the data plotted in Fig. 4, with the four units showing relatively similar thinning, but with the same trend of increasing tabularity. However, the values cannot be directly compared to those reported by Liu et al. (2018) because of the use of relative thinning rates rather than absolute ones and because Liu et al. (2018) include the mudstone caps for calculating the thinning rate.

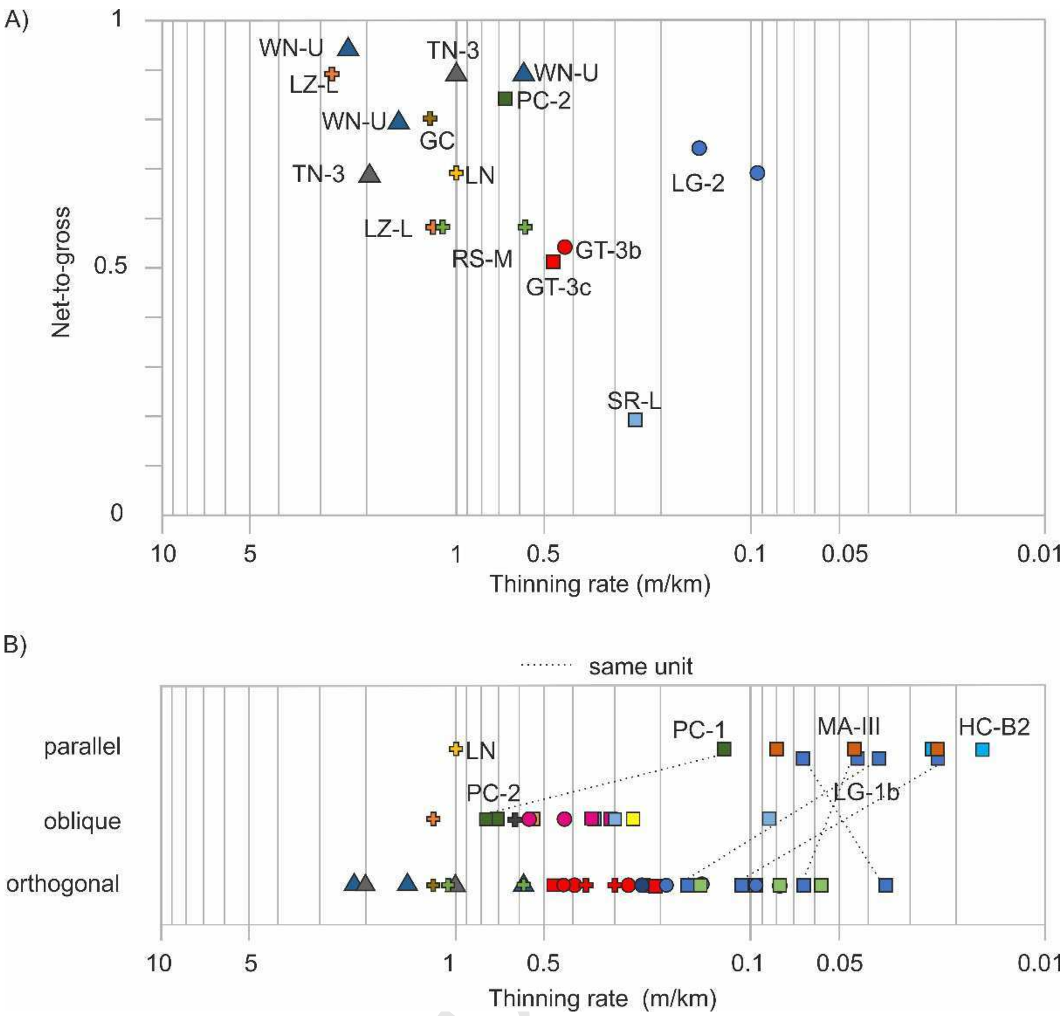

Figure 5 A) Thinning rate of 0.3-1.5 m beds for datasets with <90% beds continuity. Note that the range of thinning rate is an order of magnitude larger than for datasets with ≥90% continuous beds shown in Fig. 4B. B) Thinning rate of all datasets of 0.3-1.5 m beds plotted against the transect direction relative to palaeoflow. Dotted lines connect the measurements from the same subunit or unit, but with different transect directions. Symbols indicate the confinement index (see Fig. 4 for legend).

3.2. Tabularity and net-to-gross

The net-to-gross (sand thickness over total thickness) of most of the analysed datasets is greater than 0.5 (Fig. 4). The lowest values belong to a number of ponded (C3) systems: Tabernas (AL), Sorbas (SR-L, SR-U), Castagnola (CS-1), Marnoso-arenacea (MA-III), Hecho (HC-B2) and Las Lajas (LL). Their thinning rates are not distinct from sandier systems and within this dataset there is no relationship between thinning rate and n:g when comparing the different systems. However, the sand-rich Laga system shows especially low thinning rates and the mud-rich Tabernas and Sorbas (SR-L, SR-U, AL) especially high ones. It is suggested that this high rate of thinning recorded in the Tabernas and Sorbas basins is a result of the spatial position within the basin as the considered datasets are located ~500 m away from the basin margin (Haughton, 1994; 2001; Baudouy, 2011).

3.3. Tabularity and transect position and orientation

From a number of well-exposed large systems with high bed continuity (≥90%), it was possible to calculate sandstone bed thinning rates at two or three different positions along the system main sediment transport direction (Fig 4B,D; arrows). Beds 1.5-5 m thick are present in the Peïra Cava datasets, but not in the studied Hecho or Marnoso-arenacea datasets. The two Peïra Cava datasets (PC-2, PC-1) are 1 km apart and at different stratigraphic levels, while the three datasets for the Hecho (HC-B2) and the Marnoso-arenacea (MA-III) represent the same stratigraphic interval sampled at three locations along a proximal-to-distal 8 and 18 km long transect, respectively. They all exhibit a downstream decrease in thinning rate, coinciding with a decrease in net-to-gross. The decrease in net-to-gross might suggest that thick mudstones between sandstone beds distally can even out the topography associated with the thinning of the sandstone beds, thus removing any depositional topography and enhancing the tabularity of the next event (Remacha et al., 2005).

The transect orientation of each dataset is another variable to account for and it can help evaluate tabularity in a more three-dimensional way. Two-thirds of the datasets are measured along transects orthogonal to palaeoflow direction, one-fifth is parallel, and several others are oblique (Fig. 5B). The very low thinning rates of Marnoso-arenacea (MA-III) and Hecho (HC-B2) are probably enhanced by measuring them parallel to palaeoflow.

For some units, thinning rates are available for two transects with different orientations, allowing an evaluation of the asymmetry of tabularity measurements with respect to palaeoflow direction. In 3 out of 4 datasets of unit LG-1b, beds 0.3-1.5 m thick have lower thinning rates along dip than along strike sections, confirming the conclusions of Marini et al. (2015). In addition, two Peïra Cava datasets show a similar correlation (lower thinning rates in the section parallel to palaeoflow), albeit they belong to different stratigraphic units. An asymmetry in tabularity measurements is expected for any unconfined lobe deposit, as a function of input point, gradient and flow types. In addition, it can be speculated that the difference between continuity and thinning rates measured along strike and along dip should be correlated to the type of confinement (see Fig. 2), with frontal and lateral confinement resulting in lower tabularity along strike and along dip, respectively. However, the limited collected data and the uncertainty related to the type of confinement which characterised some of the ancient systems, did not allow direct confirmation of this hypothesis and further research is needed.

3.4. Tabularity and bed types

Two main bed types were recognised in this study: 'classical' turbidites and hybrid event beds (HEBs). The former includes Bouma-type events (complete or incomplete sequences; Bouma, 1962) and various types of 'massive' or poorly structured sandstones usually interpreted to be deposits of high density turbidity currents (Lowe, 1982; Mutti, 1992). The second group (hybrid event beds or HEBs) are beds characterised by a basal clean sandstone overlain by a mud-clast-rich argillaceous sandstone division, sometimes capped by an upper clean sandstone (Haughton et al., 2009). The formation of hybrid event beds is interpreted to be related to partial flow transformation from a turbidity current to a debris flow by en-route mud acquisition and flow partitioning (Haughton et al., 2009). The internal character and lateral facies transitions in HEBs are more complex than in turbidites and short-scale changes (metres to 100s of metres) in the beds internal make-up are common (Fonnesu et al., 2015; Pierce et al., 2018). However, the facies variations do not appear to be related to significant changes in the overall thickness of the event bed (Fonnesu et al., 2015), although some exceptions are recorded (e.g. a couple of beds from the Castagnola system; Southern et al 2015). Herein, the thinning rates of HEBs and turbidites in the same systems are compared. Note that although there is an increasing recognition of key differences between different types of HEBs (Fonnesu et al., 2018; Pierce et al., 2018), in this study all HEBs were considered together to obtain a sufficient number of beds to calculate tabularity parameters.

Hybrid event beds in the three considered cases (Gottero, Marnoso-arenacea and Castagnola) exhibit higher thinning rates than classical turbidites (between 1.3 and 2.8 times higher; Fig. 6). The Gottero (GT-3) is a HEB-rich system and in the considered distal domain around 60% of all sandstone beds are hybrid. Overall, the datasets generally demonstrate relatively high thinning rates for the mix of HEBs and turbidites present (Fig. 4). If analysed separately, HEBs are less tabular than turbidites in both thickness ranges (Fig. 6). Without HEBs, the average thinning rate would be 0.08 and 0.2 m/km lower than the average combined thinning rate for 0.3-1.5 m and 1.5-5 m beds, respectively. In the analysis, beds were considered turbidites or HEBs only based on the two chosen logs, adjacent logs were not considered. Turbidites can transition into HEBs further away. In the Castagnola (CS-1) HEBs are more abundant in the 1.5-5 m thickness range and not all datasets have both HEBs and turbidites. However, if averaged for the whole unit, the HEB thinning rate is 2.8 and 2.4 times the turbidite thinning rate for 0.3-1.5 m beds and 1.5-5 m beds, respectively. In the Marnoso-arenacea (MA-III), clean sandstones, clean to muddy sandstones and muddy sandstones have been described, interpreted as turbidites, sandy debrites and muddy debrites, respectively (Amy et al., 2005b; Amy and Talling, 2006). Due to their characteristic abrupt thinning and similar facies as HEBs, beds where either type of debritic facies was present were counted as HEBs. The thinning rate of HEBs is 1.3 times the thinning rate of turbidites in the Marnoso-arenacea. Further investigation should aim to clarify if the difference in the turbidites vs HEBs thinning rate ratio between the Gottero and the Marnoso-arenacea examples is related to different proportions of hybrid event bed types.

Although HEBs are shown to have a higher thinning rate, in all the three considered systems no clear relationship between HEB % and thinning rate between datasets of the same system was found, suggesting that other controls are dominant for overall thinning rates.

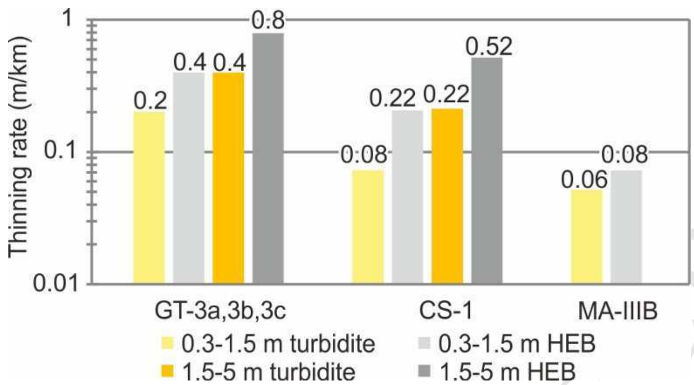

Figure 6 Thinning rates of 'classical' turbidites versus hybrid event beds for different bed thickness ranges, averaged for all datasets from each system (GT: Gottero; CS: Castagnola; MA: Marnoso-arenacea).

3.5. Tabularity vs basin size and dominant grain size

To investigate the controls on tabularity, systems that share some of their external controls should be compared. Figure 7 combines information on the average bed tabularity of each unit (both continuity and thinning rate) with their dominant grain size and inferred basin size.

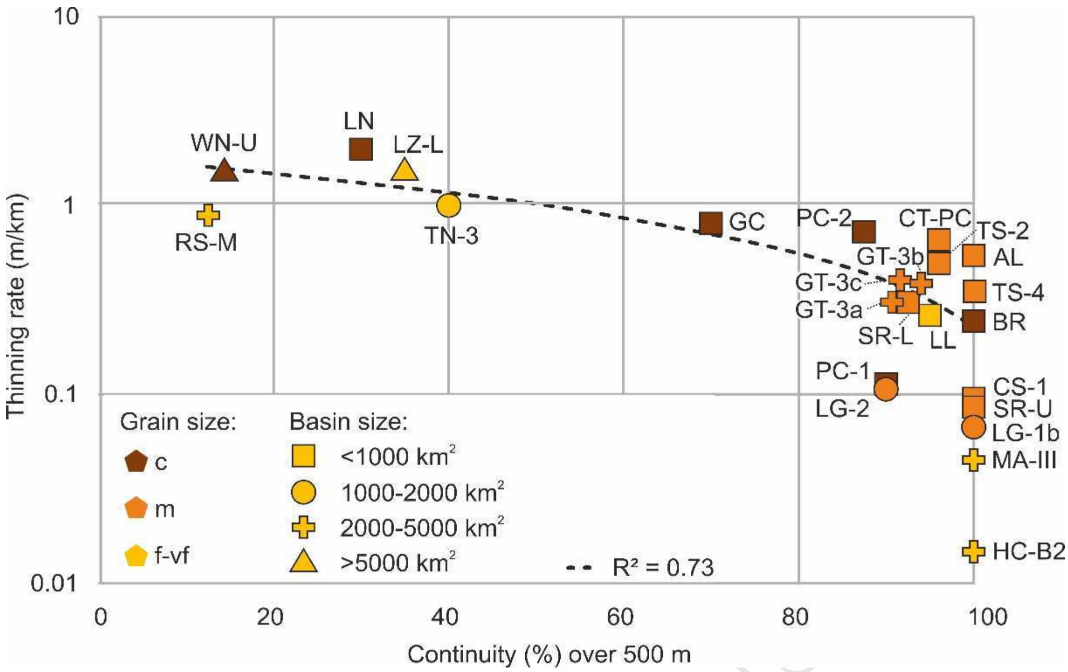

Figure 7 Relationship between bed continuity and absolute thinning rate for 0.3-1.5 m thick beds, averaged for units. Colours represent the dominant sand grain size and symbols indicate the inferred basin size (see Table 1). Dotted line is the best linear regression for all the data points.

Because of the ideal wedge geometry of a turbidite bed (Mutti, 1985; Sumner et al., 2012), the two measures of tabularity are expected to correlate and high continuity datasets should have low thinning rate. The data for beds 0.3-1.5 m thick (selected as they provide a larger data pool than for beds 1.5-5 m thick) confirm a negative linear correlation (Fig. 7).

The studied sections of the weakly confined (C1) Ross (RS-M), the ponded (C3) Marnoso-arenacea (MA-III) and the ponded (C3) Hecho (HC-B2) share the same grain size (very fine to fine sand) and the same basin size range (2000-5000 km^2). They are also characterised by the absence of 1.5-5 m beds in the studied sections. Beds are continuous for several 10s of km in the Marnoso-arenacea (MA) and the Hecho (HC), making them the most tabular systems among those considered, as opposed to a few 100s of metres in the Ross (RS). Thus, the degree of tabularity is very different, even though basin size and dominant grain size are similar, suggesting that some other external control must be at play here: perhaps the type and volume of flows entering the basins; or the proximal or distal locations, or the transect direction of the studied sections. The fine grained Tanqua Karoo (TN-3) system sits in a larger basin, its low tabularity is probably linked to its unconfined (C0) nature.

The Gottero units (GT-3a,b,c) compare to the three units mentioned above, even though they are coarser grained and comprise much thicker beds. The basin size of the Gottero is very speculative because of intense deformation and limited outcrop, but successive units point to an increasing degree of confinement (Fonnesu et al., 2018). The Gottero units show higher tabularity than the Ross (RS-M); this could be due to the higher volume flows spreading on the basin floor, which, even without full ponding in a distal setting could deposit highly tabular beds. Lower tabularity than the Marnoso-arenacea (MA-III) and the Hecho (HC-B2) could be connected to the grain size: fine grained, clay-rich, high volume flows on a low gradient basin floor can form the highest tabularity beds (Liu et al., 2018). A grain size control on tabularity may be also invoked to explain the fact that the coarse grained Windermere (WN-U) and Lauzanier (LZ-L) have higher thinning rates than the finer grained Ross, Tanqua and Laingsburg Karoo intraslope units, although it is difficult to rule out other controls. An alternative explanation is that this may be related to the presence of more beds deposited by high-concentration turbidity currents (inertia-flow type *sensu* Postma et al., 1988), in which several stages of internal bypass may occur (see Mutti, 1992). The rapid thinning might be related to the rapid depositional freezing of the basal sandy flow, while the turbulent cloud transporting the finer-grain sizes bypasses (and partially reworks) the just deposited sand. This process can result in a rapid thinning of the bed in correspondence of the flow character change (Amy et al., 2005a).

The Peïra Cava, the Braux, the Grand Coyer and the Lauzanier are all sub-basins of the same coarse grained alpine foredeep system and they are all in the range of 150-250 km^2, however, their tabularity is different. The difference could be explained by their different type of topographic confinement and distance from the sediment source: the Peïra Cava and the Braux are characterised by lateral confining slopes and could have acted as ponded depocentres, especially the Peïra Cava (Kneller & McCaffrey, 1999; Amy et al., 2007; Patacci et al., 2014); while the Grand Coyer is a channelized conduit (du Fornel et al., 2004), and the Lauzanier is a depocentre with coarser grained sediments and significant bed amalgamation (Etienne et al., 2012), suggesting a relatively more proximal setting.

4. Discussion

4.1. Quantifying tabularity

Several studies deal with quantifying the geometry of turbidite deposits using different approaches and tabularity is often discussed (e.g. Ricci Lucchi and Valmori, 1980; Pickering and Hiscott, 1985; Agirrezabala and Garcia-Mondéjar, 1994; Elliott, 2000; Cornamusini, 2004; Amy and Talling, 2006; Henstra et al., 2016). However, a consistent way to measure and report bed tabularity has not been established and many authors use the term 'tabularity' or 'sheet-like' in a descriptive and qualitative way. Some examples of quantitative characterization of thinning rates can be found in Pickering and Hilton (1998), Amy et al. (2000), Marini et al. (2015) and Liu et al. (2018). The different purpose of each study and the outcrop constrains affect the chosen lateral resolution and window of observation. Even continuous beds experience small-scale variability in thickness, owing to lateral heterogeneity in facies and in depth of erosion, or in more general, owing to the controls on thinning described earlier. Quantification of this short-scale variability assists architecture characterisation. The scale of variability investigated is different according to each study: a window <500 m captures this variability using a 25-100 m separation distance between logs as proposed by Drinkwater and Pickering (2001), while Straub and Pyles (2012) consider a 0.5 m separation over 50-700 m controlled by logs at 9-28 m spacing for calculating the coefficient of variation in deposition between two stratigraphic surfaces. Etienne et al. (2012) described lateral heterogeneity on a 10 m scale to capture bed rugosity that induces compensational stacking of successive beds. When studying large scale thinning trends, smaller scale variability is neglected, and beds can be described as lenticular in shape. Drinkwater and Pickering (2001) hypothesize that a >500 m window is more representative of topographic control, where bedsets thin toward elevated areas, rather than autogenic thinning on an even basin floor. Liu et al. (2018) consider logs separated by as little as 200 m or as far as 10 km. Marini et al. (2015) focus on lobe-scale thinning trends: their analysis of lobe scales suggests that windows >2 km should be considered. This method assumes linear decay of bed thickness, providing an estimate on lobe extent from thinning rate at smaller scale. Amy et al. (2000) also used a large, 4 km wide window; however, a bed is measured in 3 logs, which defines bed geometry more accurately than just 2 logs: convex-up, concave-up, tabular, thinning, thickening and transitional geometries can be determined.

The 500 m wide window proposed in this study sits in the middle: it does not consider very small-scale variability, but it does not average long distance measurements either. However, the possible short-scale effects due to the relatively short window are counterbalanced by taking an average over a stratigraphic interval. Absolute and relative thinning rate have been both used in previous studies. Absolute thinning rate, or simply 'thinning rate' (e.g. Marini et al., 2015) or 'thickness change factor' (Drinkwater and Pickering, 2001) allows comparison for different correlation distances. The absolute value of thickness change, neglecting the direction in which they thin, can be used, where calculating a mean value for the same bed in different sections, or different beds in the same dataset is possible. Values can also include the direction of thinning for individual beds or bedsets (usually one of the two directions possible along a correlation panel), highlighting for example compensational cycles (Drinkwater and Pickering, 2001). A symmetric lens-like geometry cancels out the thinning rate if using the mean, which is not useful for distinguishing between lenses and tabular beds. Boxplots summarizing the distribution of thickness changes of one bed between numerous log pairs can provide information on the bed geometry, on how tabular or lens-like it is (Drinkwater and Pickering, 2001).

Relative thinning rate can be normalised by mean thickness (Straub and Pyles, 2012) or thickness at a chosen location (Amy et al., 2000), but not by distance. It is useful for comparing beds belonging to different thickness range groups. Straub and Pyles (2012) used a coefficient of variation of deposit thickness to quantify aggradational versus compensational deposits. The coefficient of variation of deposit thickness expresses the variation of the ratio of the local thickness of a certain bed or bedset and the mean thickness of the same deposit over the length of the cross-section analysed. This measure is not informative on bed geometry, but only on the stacking of beds, i.e. the internal architecture of bedsets. The coefficient of variation also provides a possible quantification of scales of lateral heterogeneity: a trend of decrease of coefficient of variation (or the standard deviation) of bed thickness with increasing window of observation.

4.2. Controls on bed tabularity

Unconfined (C0) and moderately (C2) to strongly (C3) confined systems plot separately on graphs of bed continuity, with weakly (C1) confined cases having a higher data scatter (Fig. 4A,C). In the studied examples, a weak relationship exists between degree of confinement and thinning rate. A list of mechanisms through which confinement can increase bed tabularity can be considered (Fig. 8). The most effective scenario for depositing tabular beds is when both the muddy and sandy parts of the flow are ponded which implies that the thickness of event beds as well as that of their sandstone and mudstone components must scale linearly to sediment volumes discharged in the basin (Marini et al., 2016b). Flow decoupling is a common response to reflection, the dense, basal part of the flow is deflected or reflected, and the less dense finer grained part inflates as a suspension cloud (Kneller and McCaffrey, 1999; Toniolo et al., 2006; Patacci et al., 2015). The role of mud ponding on tabularity is documented in the Hecho Basin (Remacha et al., 2005), where topographic lows are preferentially filled by low continuity thin beds or mudstone caps and this likely also occurs in other systems (e.g. Peïra Cava and Castagnola; Amy et al., 2007 and Marini et al., 2016a). Ponding of the sole muddy part of a flow can also enhance tabularity. In this scenario, the sandy part of the flow might not reach the basin margin; however, the ponded mudcap can still even out the basin floor in the whole basin, and thus enhance the tabularity of the next sandstone bed. Another scenario that can enhance tabularity is ponding of the sole sandy part of the flow. This occurs when the sandy part of the flow reaches the margins and a suspension cloud fills the whole basin (Patacci et al., 2015), but the mud might overspill to a downstream basin (e.g. Unit 2 of the Castagnola system; Marini et al., 2016a). In this scenario, the sand can still be tabular due to flow ponding and likely inflation of a suspension cloud.

In the case of lateral confinement, basin margins can keep the flow uniform and at high velocity for a longer run-out distance, as opposed to letting the flow spread out and wane in an unconfined setting (Kneller, 1995). The Hecho and the Marnoso-arenacea are laterally confined as well as ponded, likely increasing flows run-out distance and bed continuity. Cross-flow tabularity appears lower than along-flow tabularity in the Laga system (Marini et al., 2015). Tectonically preformed sloping corridors with lateral, but no frontal confinement can act as bypass zones, such as in the Grand Coyer (Clark et al., 2007). In these settings, lateral confinement can channel the flows, but their highly bypassing and erosive nature will result in less tabular beds. Near confining margins, bed onlap and pinch-outs onto the slope occurs, increasing thinning rate, as shown by the relatively high thinning rate of the ponded Tabernas and Sorbas examples. Not only thinning, but also thickening type of pinch-outs (McCaffrey and Kneller, 2001) could increase the thinning rate.

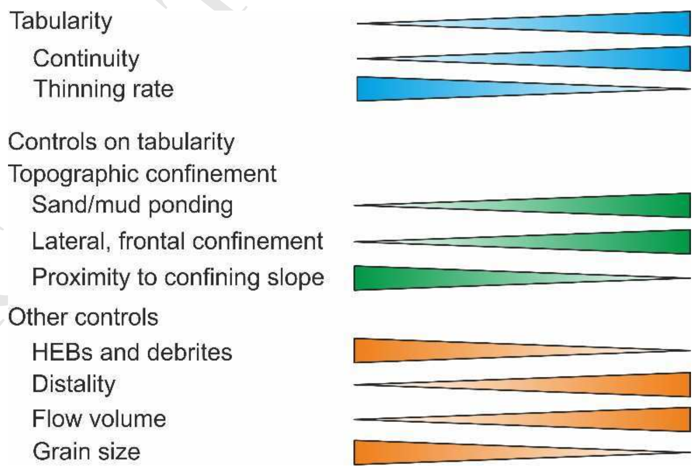

Fig. 8 Controls on tabularity. Tabularity is quantified primarily by continuity (high continuity = high tabularity) and secondarily by thinning rate (low thinning rate = high tabularity). Topographic confinement, such as the degree of sand or mud ponding and lateral or frontal confinement act as positive

controls, while proximity to confining slope are negative controls. Controls acting in confined and unconfined settings include flows volume and grain size, abundance of HEBs and debrites, distality from source area.

The presence of a higher proportion of hybrid event beds and debrites in the system decreases tabularity, although this is a minor control. These beds are characterised by rapid lateral facies changes which in some cases are coupled with thickness changes, due to the evolution of their flow rheology (e.g. Gottero, Castagnola and Marnoso-arenacea). HEBs and debrites showed 1.3-2.8 times higher thinning rates compared to turbidites in the same unit and thickness range. An additional control on local tabularity is the position of the observed point with respect to the entire length of the system. Increasing tabularity with increasing distance from the source area in long run-out systems (Marnoso-arenacea, Hecho, Peïra Cava) underlines the importance of evolving flow behaviour from more erosional to more depositional, coupled with an overall decreasing grain size and increase in grain sorting along the flow path.

Major controls on sandstone bed tabularity are flow volume and grain size, because finer grained, more efficient flows can travel farther and leave a more tabular deposit (Mutti, 1979; Liu et al., 2018). However, these controls have not been considered in isolation in this study, but only in relationship to confinement. Calculations of flow volumes and transported grain sizes (including the fraction of clay) requires very detailed dataset collected for this type of purpose, especially in unconfined systems (e.g. Jobe et al., 2018). Finally, these first order controls will be themselves the result of changes in the boundary condition or in the development stage of a turbidite system (e.g. initial, precursor flows versus an established system; flows deposited during a sea-level regression versus transgression).

The presented study dealt only with a sample of ancient systems in outcrop. However, it should be restated here that very tabular beds have been observed in present day basin-plain systems: beds from the Madeira basin plain are known to be continuous over 100-700 km, with sand correlated over 100-200 km (Stevenson et al., 2013), although only 2 out of 20 described turbidites have a maximum thickness >0.3 m. On the Cascadia margin (Adams, 1990; Nelson et al., 2000), thirteen (30-60 cm thick) seismic-triggered turbidite beds are continuous for more than 500 km downstream in the Cascadia channel, whilst one 20 cm thick turbidite is continuous for 'only' 150 km in the Astoria channel. In the Mediterranean, a megaturbidite connected to the tsunami triggered by the Crete earthquake (Polonia et al., 2016) can be correlated for >100 km; however, most of that deposit (up to 24 m) is composed of mud, while the maximum reported sand thickness is 1.3 m (Hieke and Werner, 2000). The maximum sand thickness of the Sumatran margin 2004 event is 1 m, but it is continuous for more than 200 km (Patton et al., 2015). These examples from modern systems are much more tabular compared to those studied in ancient systems. It is thought that their lack of topographic confinement, huge flow volumes and large proportion of mud result in very long run-out and consequent very high bed continuity. The bias could also be related to the fact that unconfined passive margin-type systems are usually poorly preserved in the stratigraphic record which is instead dominated by tectonically active basins in convergent or foreland-foredeep settings (Mutti et al., 2009).

5. Conclusions

Tabularity is a term commonly used in a descriptive way and refers to a range of lateral, vertical and hierarchical scales (beds and bedsets). It can be used to refer to individual beds that have a high lateral continuity and lobes are also described as tabular at certain scales. High bed tabularity has been used as an evidence of topographic confinement; however, it also characterises unconfined basin plain deposits observed in modern systems. Tabularity can be quantified on 2D transects using two variables: the percentage of beds that are continuous over a certain observation window and the thinning rate of these continuous beds. It is suggested that the terms 'tabular' or 'sheet-like' be accompanied by a quantitative characterisation of the type proposed in this paper to help comparisons between systems.

Tabularity parameters (beds continuity and thinning rates) were calculated from published log panels from eighteen ancient turbidite systems with the aim of testing the proposed methodology and the relationship between tabularity and inferred degree of confinement in these systems. Results show that all of the analysed confined and ponded basins are characterised by high bed continuity (≥90%) of the thickest beds (1.5-5 m) and by perfect continuity (100%) of medium to very thick beds (0.3-1.5 m) over a 500 m wide observation window. In contrast, the two studied unconfined systems are characterized by ≤40% bed continuity for both thickness classes. A weak relationship can be observed between degree of confinement and thinning rate, although the ranges overlap. No overall relationship can be discerned between net-to-gross and tabularity; however, in longer run-out systems, a decrease in net-to-gross is coupled with an increase in tabularity downstream. Hybrid event beds exhibit 1.3-2.8 times larger thinning rate compared to 'classical' turbidites within the same system. This suggests that HEBs presence has a negative effect (albeit minor) on overall system tabularity. Proximity to the confining slope leads to local increased thinning rates even in ponded basins. Bed continuity and thinning rate correlate, as expected, and finer grained systems generally exhibit lower thinning rates relative to coarser grained systems. Systems of comparable inferred basin size do not always share the same bed tabularity values because the concentration, volume and grain sizes of flows both absolute and relative to the basin size represent a primary factor that defines the geometry of the deposit and the degree of confinement, and therefore the resulting bed tabularity.

Acknowledgments

Financial support for a study programme at Leeds University for Lilla Tőkés was received from the Tempus Public Foundation (Campus Mundi Student Mobility) and the Papp Simon Foundation. Marco Fonnesu is thanked for providing informal feedback to an earlier version of this manuscript. We thank two anonymous reviewers for their constructive criticism that greatly improved the manuscript.

References

Adams, J., 1990. Paleoseismicity of the Cascadia Subduction Zone: Evidence from turbidites off the Oregon-Washington Margin. Tectonics 9, 569–583.

Agirrezabala, L.M., Garcia-Mondéjar, J., 1994. A coarse grained turbidite system with morphotectonic control (Middle Albian, Ondarroa, northern Iberia). Sedimentology 41, 383–407.

Albertão, G.A., Mulder, T., Eschard, R., 2011. Impact of salt-related palaeotopography on the distribution of turbidite reservoirs: Evidence from well-seismic analyses and structural restorations in the Brazilian offshore. Marine and Petroleum Geology 28, 1023–1046.

Amy, L.A., 2000. Architectural analysis of a sand-rich confined turbidite basin : the Grès de Peïra Cava, south-east France. PhD Thesis. University of Leeds.

Amy, L.A., Kneller, B., McCaffrey, W.D., 2000. Evaluating the links between turbidite characteristics and gross system architecture: upscaling insights from the turbidite sheet system of Peïra Cava, SE France. Deep-Water Reservoirs of the World, SEPM, 1–15.

Amy, L. A., Hogg, A. J., Peakall, J. and Talling, P. J., 2005a. Abrupt transitions in gravity currents. Journal of Geophysical Research-Earth Surface 110(F3).

Amy, L. A., Talling, P. J., Peakall, J., Wynn, R. B. and Thynne, R. G. A., 2005b. Bed geometry used to test recognition criteria of turbidites and (sandy) debrites. Sedimentary Geology 179, 163-174.

Amy, L.A., Talling, P.J., 2006. Anatomy of turbidites and linked debrites based on long distance (120 x 30 km) bed correlation, Marnoso Arenacea Formation, Northern Apennines, Italy. Sedimentology 53, 161–212.

Amy, L. A., Kneller, B. C. and McCaffrey, W. D., 2007. Facies architecture of the Grès de Peïra Cava, SE France: landward stacking patterns in ponded turbiditic basins. Journal of the Geological Society of London 164, 143-162.

Awadallah, S.A., Hiscott, R.N., 2004. High-resolution stratigraphy of the deep-water lower Cloridorme Formation (Ordovician), Gaspé Peninsula, based on K-bentonite and megaturbidite correlations. Canadian Journal of Earth Sciences 41, 1299–1317.

Baudouy, L., 2011. Development and evolution of a fault-controlled deep water basin - Tabernas, SE Spain (Ph.D.). University College Dublin, Dublin (413 pp.).

Booth, J.R., Dean, M.C., DuVernay III, A.E., Styzen, M.J., 2003. Paleo-bathymetric controls on the stratigraphic architecture and reservoir development of confined fans in the Auger Basin: central Gulf of Mexico slope. Marine and Petroleum Geology 20, 563–586.

Booth, J.R., DuVernay III, A.E., Pfeiffer, D.S., Styzen, M.J., 2000. Sequence stratigraphic framework, depositional models, and stacking patterns of ponded and slope fan systems in the Auger Basin: Central Gulf of Mexico slope, in: 20th Annual Research Conference, Deep-Water Reservoirs of the World, SEPM, 82–103.

Bouma, A.H., 1962. Sedimentology of some flysch deposits: a graphic approach to facies interpretation. Elsevier, Amsterdam (168 pp.).

Bruhn, C.H., Walker, R.G., 1995. High-resolution stratigraphy and sedimentary evolution of coarse-grained canyon-filling turbidites from the Upper Cretaceous transgressive megasequence, Campos Basin, offshore Brazil. Journal of Sedimentary Research 65, 17-46.

Brunt, R.L., Hodgson, D.M., Flint, S.S., Pringle, J.K., Di Celma, C., Prélat, A., Grecula, M., 2013. Confined to unconfined: Anatomy of a base of slope succession, Karoo Basin, South Africa. Marine and Petroleum Geology 41, 206–221.

Brunt, R.L., McCaffrey, W.D., Kneller, B.C., 2004. Experimental modeling of the spatial distribution of grain size developed in a fill-and-spill mini-basin setting. Journal of Sedimentary Research 74, 438–446.

Campbell, C.V., 1967. Lamina, laminaset, bed and bedset. Sedimentology 8, 7-26.

Campion, K.M., Dixon, B.T., Scott, E.D., 2011. Sediment waves and depositional implications for fine-grained rocks in the Cerro Toro Formation (upper Cretaceous), Silla Syncline, Chile. Marine and Petroleum Geology, Thematic Set on Stratigraphic Evolution of Deep-water Architecture 28, 761–784.

Carr, M., Gardner, M.H., 2000. Portrait of a Basin-Floor Fan for Sandy Deepwater Systems, Permian Lower Brushy Canyon Formation, West Texas. AAPG Memoir 72 SEPM Special Publication No 68, 215–231.

Chapin, M.A., Davies, P., Gibson, J.L., Pettingill, H.S., 1994. Reservoir architecture of turbidite sheet sandstones in laterally extensive outcrops, Ross Formation, western Ireland. Submarine Fans and Turbidite Systems, 53–68.

Clark, J., Stanbrook, D., Gardiner, A., 2007. Architecture and Facies of Confined Deep-water Clastics in the Grand Coyer Remnant, Grès d'Annot, France, in: Atlas of Deep-Water Outcrops, AAPG Studies in Geology, 181-184.

Cornamusini, G., 2004. Sand-rich turbidite system of the Late Oligocene Northern Apennines foredeep: physical stratigraphy and architecture of the "Macigno costiero"(coastal Tuscany, Italy). Geological Society of London Special Publication 222, 261–283.

Di Celma, C., Cantalamessa, G., Didaskalou, P., 2013. Stratigraphic organization and predictability of mixed coarse-grained and fine-grained successions in an upper slope Pleistocene turbidite system of the Peri-Adriatic basin. Sedimentology 60, 763–799.

Du Fornel, E., Joseph, P., Desaubliaux, G., Eschard, R., Guillocheau, F., Lerat, O., Muller, C., Ravenne, C., Sztràkos, K., 2004. The southern Grès d'Annot outcrops (French Alps): an attempt at regional correlation. Geological Society, London, Special Publications 221, 137–160.

Drinkwater, N.J., Pickering, K.T., 2001. Architectural elements in a high-continuity sand-prone turbidite system, late Precambrian Kongsfjord Formation, northern Norway: Application to hydrocarbon reservoir characterization. AAPG Bulletin 85, 1731–1757.

Elliott, T., 2000. Depositional architecture of a sand-rich, channelized turbidite system: the Upper Carboniferous Ross Sandstone Formation, western Ireland. Deep-Water Reservoirs of the World, 342–373.

Etienne, S., Mulder, T., Bez, M., Desaubliaux, G., Kwasniewski, A., Parize, O., Dujoncquoy, E., Salles, T., 2012. Multiple scale characterization of sand-rich distal lobe deposit variability: Examples from the Annot Sandstones Formation, Eocene–Oligocene, SE France. Sedimentary Geology 273–274, 1–18.

Etienne, S., Mulder, T., Razin, P., Bez, M., Désaubliaux, G., Joussiaume, R., Tournadour, E., 2013. Proximal to distal turbiditic sheet-sand heterogeneities: Characteristics of associated internal channels. Examples from the Trois Evêchés area, Eocene-Oligocene Annot Sandstones (Grès d'Annot), SE France. Marine and Petroleum Geology 41, 117–133.

Felletti, F., Bersezio, R., 2010. Quantification of the degree of confinement of a turbidite-filled basin: A statistical approach based on bed thickness distribution. Marine and Petroleum Geology 27, 515–532.

Fonnesu, M., 2016. Hybrid event bed processes, facies trends and distribution in deep-water turbidite systems. PhD thesis, University College Dublin, Ireland.

Fonnesu, M., Felletti, F., Haughton, P.D., Patacci, M., McCaffrey, W.D., 2018. Hybrid event bed character and distribution linked to turbidite system sub-environments: The North Apennine Gottero Sandstone (north-west Italy). Sedimentology 65, 151-190.

Fonnesu, M., Haughton, P., Felletti, F., McCaffrey, W., 2015. Short length-scale variability of hybrid event beds and its applied significance. Marine and Petroleum Geology 67, 583–603.

Groenenberg, R.M., Hodgson, D.M., Prélat, A., Luthi, S.M., Flint, S.S., 2010. Flow–deposit interaction in submarine lobes: insights from outcrop observations and realizations of a process-based numerical model. Journal of Sedimentary Research 80, 252–267.

Haughton, P.D., 1994. Deposits of deflected and ponded turbidity currents, Sorbas Basin, southeast Spain. Journal of Sedimentary Research 64, 233–246.

Haughton, P.D.W., 2001. Contained turbidites used to track sea bed deformation and basin migration, Sorbas Basin, south-east Spain. Basin Research 13, 117–139.

Haughton, P., Davis, C., McCaffrey, W., Barker, S., 2009. Hybrid sediment gravity flow deposits – Classification, origin and significance. Marine and Petroleum Geology 26, 1900–1918.

Henstra, G.A., Grundvåg, S.-A., Johannessen, E.P., Kristensen, T.B., Midtkandal, I., Nystuen, J.P., Rotevatn, A., Surlyk, F., Sæther, T., Windelstad, J., 2016. Depositional processes and stratigraphic architecture within a coarse-grained rift-margin turbidite system: The Wollaston Forland Group, east Greenland. Marine and Petroleum Geology 76, 187–209.

Hieke, W., Werner, F., 2000. The Augias megaturbidite in the central Ionian Sea (central Mediterranean) and its relation to the Holocene Santorini event. Sedimentary Geology 135, 205–218.

Hodgson, D.M., Flint, S.S., Hodgetts, D., Drinkwater, N.J., Johannessen, E.P., Luthi, S.M., 2006. Stratigraphic Evolution of Fine-Grained Submarine Fan Systems, Tanqua Depocenter, Karoo Basin, South Africa. Journal of Sedimentary Research 76, 20–40.

Jobe, Z.R., Howes, N., Romans, B.W., Covault, J.A., 2018. Volume and recurrence of submarine-fan-building turbidity currents. The Depositional Record. DOI: 10.1002/dep2.42.

Johnson, S.D., Flint, S., Hinds, D., De Ville Wickens, H., 2001. Anatomy, geometry and sequence stratigraphy of basin floor to slope turbidite systems, Tanqua Karoo, South Africa. Sedimentology 48, 987–1023.

Kneller, B. C., 1995. Beyond the turbidite paradigm: Physical models for deposition of turbidites and their implications for reservoir prediction. In: Hartley, A. J. and Prosser, D. J. (Eds). Characterization of Deep Marine Clastic Systems. Geological Society of London Special Publication 94: 31-49.

Kneller, B., McCaffrey, W., 1999. Depositional effects of flow nonuniformity and stratification within turbidity currents approaching a bounding slope; deflection, reflection, and facies variation. Journal of Sedimentary Research 69, 980–991.

Labourdette, R., Bez, M., 2010. Element migration in turbidite systems: Random or systematic depositional processes? AAPG Bulletin 94, 345–368.

Li, P., Kneller, B. C., Hansen, L. and Kane, I. A., 2016. The classical turbidite outcrop at San Clemente, California revisited: An example of sandy submarine channels with asymmetric facies architecture. Sedimentary Geology 346, 1-16.

Liu, Q., Kneller, B., Fallgatter, C., Buso, V.V., Milana, J.P., Baas, J., 2018. Tabularity of individual turbidite beds controlled by flow efficiency and degree of confinement. Sedimentology. DOI: 10.1111/sed.12470

Lomas, S.A., Cronin, B.T., Hartley, A.J., Duranti, D., 2007. Amalgamated sheet sandstones, Trois Eveches, France. Atlas Deep-Water Outcrops AAPG Studies in Geology 56.

Lowe, D.R., 1982. Sediment gravity flows; II, Depositional models with special reference to the deposits of high-density turbidity currents. Journal of Sedimentary Research 52, 279–297.

Marini, M., Milli, S. and Moscatelli, M., 2011. Facies and architecture of the Lower Messinian turbidite lobe complexes from the Laga Basin (central Apennines, Italy). Journal of Mediterranean Earth Sciences 3, 45-72.

Marini, M., Milli, S., Ravnås, R., Moscatelli, M., 2015. A comparative study of confined vs. semi-confined turbidite lobes from the Lower Messinian Laga Basin (Central Apennines, Italy): Implications for assessment of reservoir architecture. Marine and Petroleum Geology 63, 142–165.

Marini, M., Patacci, M., Felletti, F., McCaffrey, W.D., 2016a. Fill to spill stratigraphic evolution of a confined turbidite mini-basin succession, and its likely well bore expression: The Castagnola Fm, NW Italy. Marine and Petroleum Geology 69, 94–111.

Marini, M., Felletti, F., Milli, S., & Patacci, M. 2016b. The thick-bedded tail of turbidite thickness distribution as a proxy for flow confinement: Examples from tertiary basins of central and northern Apennines (Italy). Sedimentary Geology 341, 96-118.

McCaffrey, W., Kneller, B., 2001. Process controls on the development of stratigraphic trap potential on the margins of confined turbidite systems and aids to reservoir evaluation. AAPG Bulletin 85, 971–988.

Mueller, P., Patacci, M., Di Giulio, A., 2017. Hybrid event beds in the proximal to distal extensive lobe domain of the coarse-grained and sand-rich Bordighera turbidite system (NW Italy). Marine and Petroleum Geology 86, 908–931.

Mutti, E., 1977. Distinctive thin-bedded turbidite facies and related depositional environments in the Eocene Hecho Group (South-central Pyrenees, Spain). Sedimentology 24, 107–131.

Mutti, E., 1979. Turbidites et cones sous-marins profonds, in Peter Homewood (Ed.), Sedimentation Detritique (Fluviatile, Littorale et Marine), Institut de Geologie, Universite de Fribourg, Suisse, pp. 353-419.

Mutti, E., 1985. Turbidite systems and their relations to depositional sequences, in: Provenance of Arenites. Springer, pp. 65–93.

Mutti, E., 1992. Turbidite sandstones. San Donato Milanese, Agip, 275 p.

Mutti, E., Bernoulli, D., Ricci Lucchi, F. and Tinterri, R., 2009. Turbidites and turbidity currents from Alpine 'flysch' to the exploration of continental margins. Sedimentology 56(1): 267-318.

Muzzi Magalhaes, P., Tinterri, R., 2010. Stratigraphy and depositional setting of slurry and contained (reflected) beds in the Marnoso-arenacea Formation (Langhian-Serravallian) Northern Apennines, Italy. Sedimentology 57, 1685–1720.

Nelson, C.H., Goldfinger, C., Johnson, J.E., Dunhill, G., 2000. Variation of modern turbidite systems along the subduction zone margin of Cascadia Basin and implications for turbidite reservoir beds, in: Deep-Water Reservoirs of the World: Gulf Coast Section, SEPM, Annual Research Conference, CD ROM. pp. 714–738.

Patacci, M., 2016. A high-precision Jacob's staff with improved spatial accuracy and laser sighting capability. Sedimentary Geology 335, 66–69.

Patacci, M., Haughton, P.D.W., McCaffrey, W.D., 2014. Rheological complexity in sediment gravity flows forced to decelerate against a confining slope, Braux, SE France. Journal of Sedimentary Research 84, 270–277.

Patacci, M., Haughton, P.D.W., McCaffrey, W.D., 2015. Flow Behavior of Ponded Turbidity Currents. Journal of Sedimentary Research 85, 885–902.

Patton, J.R., Goldfinger, C., Morey, A.E., Ikehara, K., Romsos, C., Stoner, J., Djadjadihardja, Y., Ardhyastuti, S., Gaffar, E.Z., Vizcaino, A., others, 2015. A 6600 year earthquake history in the region of the 2004 Sumatra-Andaman subduction zone earthquake. Geosphere 11, 2067–2129.

Pickering, K. T. and Hilton, V. C., 1998. Turbidite Systems of SE France. London, Vallis Press, 229 p.

Pickering, K.T., Hiscott, R.N., 1985. Contained (reflected) turbidity currents from the Middle Ordovician Cloridorme Formation, Quebec, Canada: an alternative to the antidune hypothesis. Sedimentology 32, 373–394.

Pickering, K., Hiscott, R., 2015. Deep Marine Systems: Processes, Deposits, Environments, Tectonic and Sedimentation. John Wiley & Sons, (672 pp.).

Pierce, C.S., Haughton, P.D.W., Shannon, P.M., Pulham, A.J., Barker, S.P., Martinsen, O.J., Baas, J., 2018. Variable character and diverse origin of hybrid event beds in a sandy submarine fan system, Pennsylvanian Ross Sandstone Formation, western Ireland. Sedimentology 65, 952–992.

Polonia, A., Vaiani, S.C., de Lange, G.J., 2016. Did the AD 365 Crete earthquake/tsunami trigger synchronous giant turbidity currents in the Mediterranean Sea? Geology 44, 191–194.

Postma, G., Nemec, W., Kleinspehn, K.L., 1988. Large Floating Clasts in Turbidites: A Mechanism for Their Emplacement. Sedimentary Geology 58, 47-61.

Prather, B.E., Booth, J.R., Steffens, G.S., Craig, P.A., 1998. Classification, lithologic calibration, and stratigraphic succession of seismic facies of intraslope basins, deep-water Gulf of Mexico. AAPG Bulletin 82, 701–728.

Remacha, E., Fernández, L.P., 2003. High-resolution correlation patterns in the turbidite systems of the Hecho Group (South-Central Pyrenees, Spain). Marine and Petroleum Geology 20, 711–726.

Remacha, E., Fernandez, L.P., Maestro, E., 2005. The Transition Between Sheet-Like Lobe and Basin-Plain Turbidites in the Hecho Basin (South-Central Pyrenees, Spain). Journal of Sedimentary Research 75, 798–819.

Ricci Lucchi, F., Valmori, E., 1980. Basin-wide turbidites in a Miocene, over-supplied deep-sea plain: a geometrical analysis. Sedimentology 27, 241–270.

Saller, A., Werner, K., Sugiaman, F., Cebastiant, A., May, R., Glenn, D., Barker, C., 2008. Characteristics of Pleistocene deep-water fan lobes and their application to an upper Miocene reservoir model, offshore East Kalimantan, Indonesia. AAPG Bulletin 92, 919–949.

Sinclair, H.D., Tomasso, M., 2002. Depositional evolution of confined turbidite basins. Journal of Sedimentary Research 72, 451–456.

Slatt, R.M., Stone, C.G., Weimer, P., 2000. Characterization of slope and basin facies tracts, Jackfork Group, Arkansas, with applications to deepwater (turbidite) reservoir management, in: Deep-Water Reservoirs of the World: 20th Annual Bob F. Perkins Research Conference, Gulf Coast Section-SEPM. SEPM, pp. 87–103.

Smith, R. and Joseph, P., 2004. Onlap stratal architectures in the Gres d'Annot: geometric models and controlling factors,in: Joseph, P. and Lomas, S. A. (Eds). Deep-Water Sedimentation in the Alpine Basin of SE France: New Perspectives on the Gres D'Annot and Related Systems. Geological Society of London Special Publication 221, pp. 389-399.

Southern, S.J., 2015. Influence of basin physiography upon the evolution and sedimentation from flows transitional between turbidity current and debris flow. PhD Thesis, University of Leeds.

Southern, S.J., Patacci, M., Felletti, F., McCaffrey, W.D., 2015. Influence of flow containment and substrate entrainment upon sandy hybrid event beds containing a co-genetic mud-clast-rich division. Sedimentary Geology 321, 105–122.

Spychala, Y.T., Hodgson, D.M., Flint, S.S., Mountney, N.P., 2015. Constraining the sedimentology and stratigraphy of submarine intraslope lobe deposits using exhumed examples from the Karoo Basin, South Africa. Sedimentary Geology 322, 67–81.

Stevenson, C.J., Talling, P.J., Wynn, R.B., Masson, D.G., Hunt, J.E., Frenz, M., Akhmetzhanhov, A., Cronin, B.T., 2013. The flows that left no trace: Very large-volume turbidity currents that bypassed sediment through submarine channels without eroding the sea floor. Marine and Petroleum Geology 41, 186–205.

Straub, K.M., Pyles, D.R., 2012. Quantifying the hierarchical organization of compensation in submarine fans using surface statistics. Journal of Sedimentary Research 82, 889–898.

Sumner, E.J., Talling, P.J., Amy, L.A., Wynn, R.B., Stevenson, C.J., Frenz, M., 2012. Facies architecture of individual basin-plain turbidites: Comparison with existing models and implications for flow processes. Sedimentology 59, 1850–1887.

Terlaky, V., Arnott, R.W.C., 2014. Matrix-rich and associated matrix-poor sandstones: Avulsion splays in slope and basin-floor strata. Sedimentology 61, 1175–1197.

Terlaky, V., Rocheleau, J., Arnott, R.W.C., 2016. Stratal composition and stratigraphic organization of stratal elements in an ancient deep-marine basin-floor succession, Neoproterozoic Windermere Supergroup, British Columbia, Canada. Sedimentology 63, 136–175.

Talling, P.J., Malgesini, G., Felletti, F., 2012. Can liquefied debris flows deposit clean sand over large areas of sea floor? Field evidence from the Marnoso-arenacea Formation, Italian Apennines. Sedimentology 60, 720–762.Tinterri, R., Tagliaferri, A., 2015. The syntectonic evolution of foredeep turbidites related to basin segmentation: Facies response to the increase in tectonic confinement (Marnoso-arenacea Formation, Miocene, Northern Apennines, Italy). Marine and Petroleum Geology 67, 81–110.

Toniolo, H., Lamb, M., Parker, G., 2006. Depositional Turbidity Currents in Diapiric Minibasins on the Continental Slope: Formulation and Theory. Journal of Sedimentary Research 76, 783–797.

Weimer, P., Slatt, R.M., 2006. Introduction to the Petroleum Geology of Deepwater Settings, AAPG Studies in Geology 57, (816 pp.).

Novel methodology for quantifying tabularity based on bed continuity and bed thinning

Tabularity values from published studies of eighteen ancient turbidite systems

In the studied systems bed continuity is higher in confined systems

Quantitative determination of tabularity should become a standard workflow in outcrop